

# UCLA

## UCLA Previously Published Works

### Title

Method for live-cell super-resolution imaging of mitochondrial cristae and quantification of submitochondrial membrane potentials

### Permalink

<https://escholarship.org/uc/item/0vt624fr>

### Authors

Wolf, Dane M  
Segawa, Mayuko  
Shirihai, Orian S  
et al.

### Publication Date

2020

### DOI

10.1016/bs.mcb.2019.12.006

Peer reviewed



Published in final edited form as:

*Methods Cell Biol.* 2020 ; 155: 545–555. doi:10.1016/bs.mcb.2019.12.006.

## Method for live-cell super-resolution imaging of mitochondrial cristae and quantification of submitochondrial membrane potentials

Dane M. Wolf<sup>a,b,c,†</sup>, Mayuko Segawa<sup>a,b,†</sup>, Orian S. Shirihai<sup>a,b,\*</sup>, Marc Liesa<sup>a,b,d,\*</sup>

<sup>a</sup>Department of Medicine, Endocrinology, David Geffen School of Medicine, University of California Los Angeles, Los Angeles, CA, United States

<sup>b</sup>Department of Molecular and Medical Pharmacology, David Geffen School of Medicine, University of California Los Angeles, Los Angeles, CA, United States

<sup>c</sup>Graduate Program in Nutrition and Metabolism, Graduate Medical Sciences, Boston University School of Medicine, Boston, MA, United States

<sup>d</sup>Molecular Biology Institute, University of California Los Angeles, Los Angeles, CA, United States

### Abstract

The emergence of diffraction-unlimited live-cell imaging technologies has enabled the examination of mitochondrial form and function in unprecedented detail. We recently developed an approach for visualizing the inner mitochondrial membrane and determined that cristae membranes possess distinct mitochondrial membrane potentials, representing unique bioenergetic sub-domains within the same organelle. Here, we outline a methodology for resolving cristae and inner boundary membranes using the LSM880 with Airyscan. Furthermore, we demonstrate how to analyze TMRE fluorescence intensity using the Nernst equation to calculate membrane potentials of individual cristae. Altogether, using these new techniques to study the electrochemical properties of the cristae can help to gain deeper insight into the still elusive nature of the mitochondrion.

### 1 Rationale

Historically, diffraction limits of light microscopes have prevented the resolution of mitochondrial ultrastructure in living cells (Jakobs & Wurm, 2014). Recent advancements in high- and super-resolution microscopy—e.g., Airyscan microscopy (Wolf et al., 2019), stimulated emission depletion (STED) microscopy (Kondadi et al., 2019; Stephan, Roesch, Riedel, & Jakobs, 2019; Wang et al., 2019), and structured illumination microscopy (SIM) (Huang et al., 2018)—have enabled the visualization of the inner mitochondrial membrane (IMM) in real time. Here, we outline the novel approach for imaging the IMM using the Zeiss LSM880 with Airyscan. This technique is advantageous because the lateral resolution

\*Corresponding authors: oshirihai@mednet.ucla.edu; mliesa@mednet.ucla.edu.

†These authors contributed equally to this study.

Conflict of interest

The authors declare that they have no conflicts of interest.

of the Airyscan system is 140 nm, better than that obtained using a confocal laser scanning microscope. As a result, it can be used to visualize both cristae as well as the inner boundary membrane (IBM) in live cells, using various dyes that label the IMM. We further provide a step-by-step protocol for obtaining a functional readout of the membrane potential ( $\Psi_m$ ) heterogeneity associated with different segments of the IMM, as first described in Wolf et al. (2019). Quantifying different membrane potentials associated with individual cristae provides a new parameter for evaluating mitochondrial function in health and disease (Wolf et al., 2019).

## 2 Materials, equipment and reagents

### 2.1 Cell culture

HeLa cells were grown in DMEM (12100-046), supplemented with sodium bicarbonate, HEPES, Pen/Strep, sodium pyruvate, and 10% FBS and cultured in 5% CO<sub>2</sub> at 37 °C. H1975 cells were cultured in RPMI-1640 media (31800-022), supplemented with sodium bicarbonate, sodium pyruvate, HEPES, Pen/Strep, and 10% FBS and grown in 5% CO<sub>2</sub> at 37 °C.

### 2.2 Reagents and equipment for live-cell Airyscan imaging

CELLview 4-compartment glass-bottom tissue culture dishes, PS, 35/10 mm (Greiner Bio-One, 627870) were utilized for plating/imaging cells. Cells were stained with 10-*N*-nonyl acridine orange (NAO) (100 nM) and/or tetramethylrhodamine, ethyl ester (TMRE) (15 nM) 1 h prior to live-cell imaging. Image acquisition was performed with the alpha Plan-Apochromat 100x/1.46 Oil DIC M27 objective on the Zeiss LSM 880 with Airyscan (Huff, 2015). Raw.czi files were processed automatically into decon-volved images using the Airyscan processing in the ZEN software.

### 2.3 Image preparation

Processed Airyscan images were analyzed using ImageJ (Fiji) software (Schindelin et al., 2012). Briefly, before cropping cells and performing any analysis, background was subtracted from images using a rolling ball filter  $\frac{1}{4}$  50. For representative images, we used the Window/Level function if showing relevant changes in pixel intensities; if comparing cellular structures, we adjusted pixel intensities to optimally demonstrate relevant differences in mitochondrial architecture.

## 3 Protocols

Visualization of IMM structure in living cells:

1. Plate cells in an imaging dish.
2. Culture at least 24 h, or until cells adhere and spread out on the plate.
3. Stain cells with 10-*N*-nonyl acridine orange (NAO) at a concentration of 100 nM.
4. After incubating 1 h, replace NAO-containing media with normal cell-culture media.

5. Turn on microscope (LSM880 with Airyscan), open ZEN software, and turn on laser(s)—e.g., 488-nm argon (Coherent).
6. Bring cells to microscope, and position in the incubation chamber, previously set to 37 °C.
7. Adjust objective to the alpha Plan-Apochromat 100 x/1.46 Oil DIC M27.
8. Using brightfield, bring cells into focus.
9. Adjust beam splitter to MBS 488, set 488-nm laser power between approximately 0.3% and 2.4%.
10. Select the BP 495–550 + LP 570 (or other compatible) filter.
11. Set master gain between 850 and 900.
12. Begin continuous scanning at maximum speed at a zoom factor of 0.6. *Note:* NAO is susceptible to rapid photobleaching, so adjust the laser power/gain while zoomed out all the way to minimize photobleaching.
13. After obtaining a relatively strong signal-to-noise ratio, bring a field of mitochondria into focus and stop scanning.
14. Select a cell or region of a cell, and use the crop function to zoom in around 2.5–9.0 x.
15. Set pixel dwell between 4.12 and 9.15  $\mu$ s, respectively.
16. Acquire image. Save.

Visualization of mitochondrial membrane potential ( $\Psi_m$ ) at cristae and IBM:

1. Follow the steps outlined above for NAO but include the dye tetramethylrhodamine, ethyl ester (TMRE) in the media at a concentration of 15 nM. Incubate cells with NAO and TMRE for 1 h. Replace the media containing NAO and TMRE with media containing only 15 nM TMRE. *Note:* if NAO is left in the media for an extended period of time, it can result in mitochondrial swelling.
2. In addition to the microscope settings indicated in the preceding section for visualization of the IMM, adjust the beam splitter to MBS 488/561, and set 561-nm laser power between approximately 0.2% and 0.5%. *Note:* it is important to keep the laser power as low as possible in order to prevent bleed-through. To ascertain that bleed-through is not occurring, image wells with only NAO or only TMRE and excite with both 488- and 561-nm lasers. Under these conditions, choose a laser power where the 561-nm laser does not result in excitation/emission (ex/em) of the NAO, and the 488-nm laser does not result in ex/em of the TMRE. This will verify that any signals in the green (NAO) and red (TMRE) channels correspond to structural and functional information, respectively (Wolf et al., 2019).

Methods for calculating membrane potentials (Ehrenberg, Montana, Wei, Wuskell, & Loew, 1988; Farkas, Wei, Febroriello, Carson, & Loew, 1989; Loew, Tuft, Carrington, & Fay,

1993; Twig et al., 2008, 2010; Wikstrom et al., 2007; Wolf et al., 2019) within submitochondrial compartments (Wolf et al., 2019): To compare the  $\Psi$  along the main segments of the IMM—i.e., cristae and IBM—measure and record the fluorescence intensities (FIs) of TMRE associated with cristae, nearby IBM, and matrix. After opening an Airyscan image of mitochondria in ImageJ (Fiji), hold cursor over a specific crista, and record in Excel the associated FI of the TMRE channel in the status bar of the main window of ImageJ. Then hold the cursor over a nearby region of IBM contiguous with this crista, and record in Excel its associated FI, as described above. Repeat this process for dimmer regions between cristae and IBM, which are mitochondrial matrix. *Note:* in WT cells, the FI associated with cristae tends to be higher than that of IBM. Record measurements of multiple cristae, IBM, and matrix across a single mitochondrion to obtain values for submitochondrial  $\Psi$  heterogeneity (Wolf et al., 2019).

1. Apply the Nernst equation:

$$\Delta\Psi_m = (RT)\log(FI_{\text{comp1}}/FI_{\text{comp2}})$$

where,  $RT=(\text{gas constant})(\text{temperature})=61.5$  and  $FI_{\text{comp}} = \text{Fluorescence intensity of specific compartment}$ .

2. To quantify the membrane potentials of cristae and IBM relative to the membrane potential of the whole mitochondrion, plug in the FI values for cristae or IBM into the numerator and the FI values for the whole mitochondrion (i.e.,  $FIMito = \text{average of cristae, IBM, and matrix FIs}$ ) into the denominator of the log function:

$$\Delta\Psi_{\text{Cr-Mito}} = (RT)\log(FI_{\text{Cr}}/FI_{\text{Mito}}) = (61.5)\log(FI_{\text{Cr}}/FI_{\text{Mito}})$$

$$\Delta\Psi_{\text{IBM-Mito}} = (RT)\log(FI_{\text{IBM}}/FI_{\text{Mito}}) = (61.5)\log(FI_{\text{IBM}}/FI_{\text{Mito}})$$

3. The above formulation underestimates the intensity of the membrane potential at the cristae, because it references the average FI of the whole mitochondrion, which includes the high-intensity pixels at the cristae. It is more accurate, therefore, to directly reference the FIs associated with cristae to those of the IBM:

$$\Delta\Psi_{\text{Cr-IBM}} = (RT)\log(FI_{\text{Cr}}/FI_{\text{IBM}}) = (61.5)\log(FI_{\text{Cr}}/FI_{\text{IBM}})$$

4. When performing a perturbation, compare the  $\Psi_{\text{Cr-IBM}}$  of treatment with that of control. Alterations in the activity of the respiratory chain and/or the structure of the IMM are likely to result in physiologically relevant changes in the polarity of cristae, as determined by calculating the  $\Psi_{\text{Cr-IBM}}$  (Wolf et al., 2019). See figures for additional details.

## 4 Safety considerations and standards

Researchers planning to use these techniques should first obtain appropriate biological and laser-safety trainings associated with their respective institutions. Users must exercise particular caution when using Class 3B and Class 4 lasers, as they represent serious risks for eye and/or skin damage.

## 5 Analysis and statistics

Diffraction limits associated with conventional light microscopy have prevented the resolution of the IMM in living cells. As a result, mitochondria stained with different dyes have appeared as “thread-” or “grain-like” structures, giving off relatively uniform fluorescence intensity. However, state-of-the-art high- and super-resolution microscopes are now capable of revealing the internal complexities of the IMM in real time (Huang et al., 2018; Kondadi et al., 2019; Stephan et al., 2019; Wang et al., 2019; Wolf et al., 2019). Using the LSM880 with Airyscan, we show that it is possible to resolve both the cristae as well as the IBM in living cells (Fig. 1A and B) (Wolf et al., 2019). As demonstrated by electron micrographs, the IMM consists of numerous crest-like structures—i.e., “cristae”—typically oriented in a perpendicular manner to the long axis of the mitochondrion (Palade, 1953). Using the latest live-cell fluorescence imaging technologies, they appear as thin lines with a width of approximately 50–100 nm and a length of around 200–700 nm. The cristae appear separated from each other by dimmer regions, which we previously identified as mitochondrial matrix (Wolf et al., 2019). Adjoining the ends of the cristae, the IBM is visible as a thin line running parallel to the long axis of the mitochondrion. Note that, in spite of the improved resolution of Airyscan and other advanced imaging technologies, these systems still cannot resolve mitochondrial ultrastructure as accurately as electron microscopy; therefore, objects, such as cristae, will continue to appear larger than their actual size. When interpreting live-cell images of the IMM, analysts should remain cognizant of the possibility that a relatively large intramitochondrial structure could represent multiple, closely apposed cristae, which cannot be clearly resolved.

We recently demonstrated that cristae possess unique bioenergetic properties— i.e., that the  $\Psi_m$  is not uniformly distributed along the IMM, but that it varies in intensity such that regions with higher  $\Psi_m$  are associated with cristae rather than IBM (Wolf et al., 2019). Furthermore, we determined that different cristae can display significantly different membrane potentials from one another (Wolf et al., 2019). These findings point to a new parameter that can be measured when assessing mitochondrial function. For example, images of a HeLa cell, stained with NAO and TMRE (Fig. 2A–C), show that the  $\Psi_m$  (TMRE) displays a heterogeneous pattern along the IMM, with most intense signals colocalizing with cristae compared to IBM. Since we identified that alterations in mitochondrial ultrastructure can impinge upon the function of cristae as independent bioenergetic units (Wolf et al., 2019), it is now relevant to ask not only how different perturbations may affect the membrane potential of the entire organelle ( $\Psi_m$ ) but also how they affect the membrane potentials of the individual cristae ( $\Psi_{Cr}$ ). Intriguingly, we found that perturbations in proteins that regulate crista junctions (CJs) and/or mitochondrial dynamics can result in hypo- and/or hyper-polarization. Hypo-polarization tended to be

associated with compromising the integrity of CJs, which appear to normally play a role in electrically insulating cristae from adjoining IBM. Conversely, hyper-polarization tended to result from detachment of cristae from IBM, forming intramitochondrial vesicular structures (Wolf et al., 2019). To quantify differences in  $\Psi$  between the principal segments of the IMM (i.e., the cristae and IBM), an analyst can measure the TMRE FI at different compartments and apply the Nernst equation (Fig. 2D), as described in the protocol above. In unperturbed cells, the  $\Psi_{Cr}$  tends to be significantly higher and the membrane potential of the IBM ( $\Psi_{IBM}$ ) tends to be significantly lower than that of the whole mitochondrion ( $\Psi_{Mito}$ ). It is important to note, however, that calculating the  $\Psi_{Cr}$  relative to the  $\Psi_{Mito}$  underestimates the actual value. Therefore, when examining possible changes in  $\Psi_{Cr}$  after performing a perturbation, it is more accurate to compare the membrane potential of the cristae relative to the nearby IBM ( $\Psi_{Cr-IBM}$ ).

To determine whether there are statistically significant differences in the membrane potentials associated with cristae, analysts should first evaluate whether the data are normally distributed and perform parametric or nonparametric two-tailed *t*-tests, accordingly.

## 6 Pros and cons

Pros	Cons
Use of conventional dyes like NAO, TMRE, MTG allow visualization of IMM in living cells	Dyes tend to photobleach rapidly compared to fluorescent proteins, such as GFP
Airyscan is less likely to result in photobleaching compared to STED	Airyscan has lower resolution than STED or SIM
Airyscan permits quantification of membrane potential at cristae in addition to that of the whole organelle	Analysis of membrane potential at cristae involves additional analysis, which is more time-consuming if not subjected to automation

## 7 Troubleshooting and optimization

Problem	Solution
Mitochondrial swelling as a result of incubation with NAO	Decrease NAO incubation time
Difficulty resolving cristae	Make sure there is sufficient signal to noise; ascertain that mitochondria are in focus; adjust pixel dwell; zoom in more closely on area of mitochondrial network; use 100 × oil objective
Mitochondria depolarize while imaging, as indicated by a loss of TMRE fluorescence intensity	Turn down laser power and/or increase scanning speed

Note: *depending on variations in cell type, imaging systems, etc., users should attempt to optimize these settings, accordingly.*

## 8 Summary

Here, we summarize a novel protocol for imaging cristae and IBM in living cells, using Airyscan technology. Furthermore, we show a detailed description of how to employ the  $\Psi_m$ -dependent dye, TMRE, to visualize and measure different membrane potentials

associated with cristae and IBM. Our observation that cristae are relatively autonomous bioenergetic units (Wolf et al., 2019) raises many new questions as to how the structure and function of cristae impact health and disease. Future studies aimed at addressing the functional role of cristae in living cells can benefit from the methods outlined above.

## Acknowledgments

We would like to thank Dr. David Nicholls, Dr. David Shackelford, Dr. Alexander van der Bliek, Dr. Andreas Reichert, Dr. Paolo Bernardi for valued discussions that helped us develop these approaches. We would like to thank Dr. Daniel Dagan for his help in reviewing this manuscript and providing criticism and comments. We would like to thank Dion Baybridge for his continued and valued support of the graduate students on our team. O.S.S. is funded by NIH-NIDDK 5-RO1DK099618-02. M.L. and M.S. are funded by UCLA Department of Medicine Chair commitment, UCSD/UCLA Diabetes Research Center grant, NIH P30 DK063491 and 1R01AA026914-01A1.

## References

- Ehrenberg B, Montana V, Wei M, Wuskell JP, & Loew LM (1988). Membrane potential can be determined in individual cells from the Nernstian distribution of cationic dyes. *Biophysical Journal*, 53, 785–794. [PubMed: 3390520]
- Farkas DL, Wei M, Febroriello P, Carson JH, & Loew LM (1989). Simultaneous imaging of cell and mitochondrial membrane potentials. *Biophysical Journal*, 56, 1053–1069. [PubMed: 2611324]
- Huang X, Fan J, Li L, Liu H, Wu R, Wu Y, et al. (2018). Fast, long-term, super-resolution imaging with Hessian structured illumination microscopy. *Nature Biotechnology*, 36, 451–459.
- Huff J (2015). The Airyscan detector from ZEISS: Confocal imaging with improved signal- to-noise ratio and super-resolution. *Nature Methods*, 12, i–ii.
- Jakobs S, & Wurm CA (2014). Super-resolution microscopy of mitochondria. *Current Opinion in Chemical Biology*, 20, 9–15. [PubMed: 24769752]
- Kondadi AK, Anand R, Hansch S, Urbach J, Zobel T, Wolf DM, et al. (2019). Cristae undergo cycles of fusion and fission in MICOS-dependent manner. *BioRxiv*.
- Loew LM, Tuft RA, Carrington W, & Fay FS (1993). Imaging in five dimensions: Time-dependent membrane potentials in individual mitochondria. *Biophysical Journal*, 65, 2396–2407. [PubMed: 8312478]
- Palade GE (1953). An electron microscope study of the mitochondrial structure. *The Anatomical Record*, 114, 427–452. 1952.
- Schindelin J, Arganda-Carreras I, Frise E, et al. (2012). Fiji: An open-source platform for biological-image analysis. *Nature Methods*, 9, 676–682. 10.1038/nmeth.2019. [PubMed: 22743772]
- Stephan T, Roesch A, Riedel D, & Jakobs S (2019). Live-cell STED nanoscopy of mitochondrial cristae. *Scientific Reports*, 9, 12419. [PubMed: 31455826]
- Twig G, Elorza A, Molina AJ, Mohamed H, Wikstrom JD, Walzer G, et al. (2008). Fission and selective fusion govern mitochondrial segregation and elimination by autophagy. *The EMBO Journal*, 27, 433–446. [PubMed: 18200046]
- Twig G, Liu X, Liesa M, Wikstrom JD, Molina AJ, Las G, et al. (2010). Biophysical properties of mitochondrial fusion events in pancreatic beta-cells and cardiac cells unravel potential control mechanisms of its selectivity. *American Journal of Physiology. Cell Physiology*, 299, C477–C487. [PubMed: 20445168]
- Wang C, Taki M, Sato Y, Tamura Y, Yaginuma H, Okada Y, et al. (2019). A photostable fluorescent marker for the superresolution live imaging of the dynamic structure of the mitochondrial cristae. *PNAS*, 116, 15817–15822. [PubMed: 31337683]
- Wikstrom JD, Katzman SM, Mohamed H, Twig G, Graf SA, Heart E, et al. (2007). Beta-cell mitochondria exhibit membrane potential heterogeneity that can be altered by stimulatory or toxic fuel levels. *Diabetes*, 56, 2569–2578. [PubMed: 17686943]
- Wolf DM, Segawa M, Kondadi AK, Anand R, Bailey ST, Reichert AS, et al. (2019). Individual cristae within the same mitochondrion display different membrane potentials and are functionally independent. *The EMBO Journal*, 38, e101056. [PubMed: 31609012]

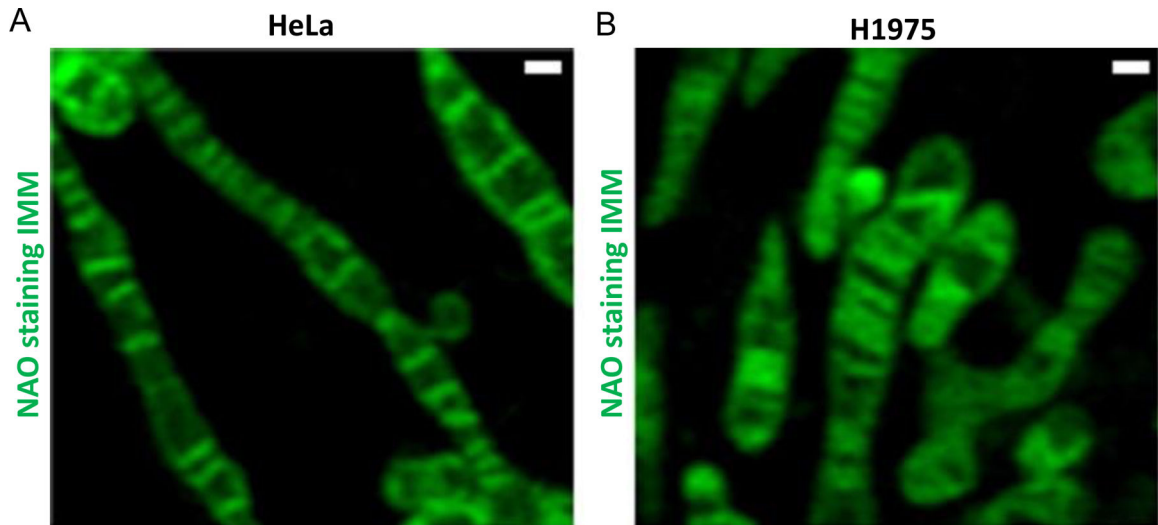


**FIG. 1.**

Airyscan imaging technology can resolve the inner mitochondrial membrane (IMM) in living cells. Live-cell Airyscan images of different cell types showing resolution of IMM. (A) Image of IMM in a HeLa cell stained with NAO. Scale bar=4500 nm. White and blue arrowheads indicate cristae and IBM, respectively. Note: the dimmer regions between cristae are mitochondrial matrix.  $N=3$  independent experiments. (B) Image of IMM in H1975 cell stained with NAO. Scale bar=500 nm. White and blue arrowheads indicate cristae and IBM, respectively. Note: the dimmer regions between cristae are mitochondrial matrix.  $N=3$  independent experiments.

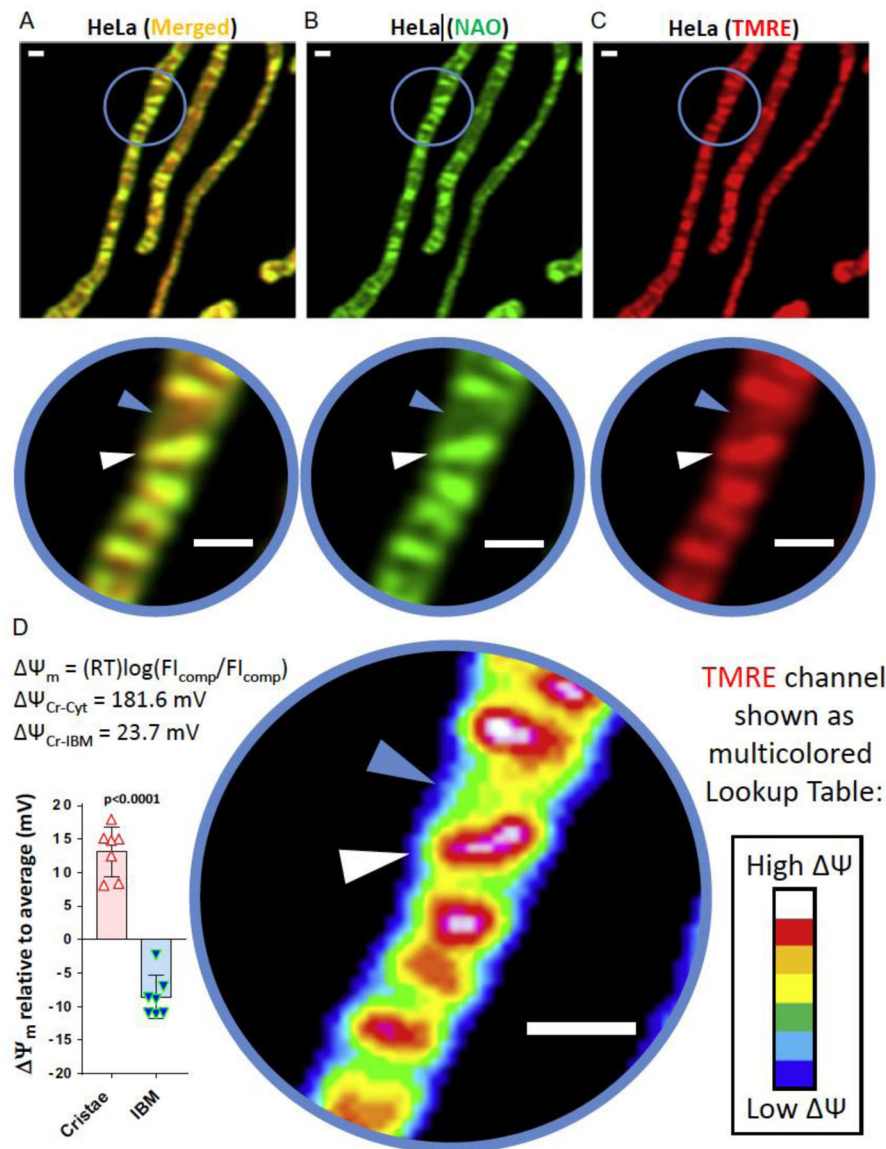


**FIG. 2.** Method for obtaining structural and functional information associated with cristae in real time. Live-cell Airyscan images of HeLa cell showing real-time, function-structure read-outs. (A) Live-cell Airyscan image of a HeLa cell co-stained with NAO and TMRE, showing higher membrane potential associated with cristae. Scale bar=500nm. Blue circle marks zoomed-in region below image, where white and blue arrowheads indicate crista and IBM, respectively. Scale bar=500nm. (B) Green channel (NAO) from (A) shows cristae and IBM architecture. Scale bar=500nm. Blue circle marks zoomed-in region below image, where white and blue arrowheads indicate crista and IBM, respectively. Scale bar= 500 nm.(C) Red channel (TMRE) from (A) shows heterogeneity in  $\Psi_m$  associated with different mitochondrial subdomains. Scale bar=500nm. Blue circle marks zoomed-in region below image, where white and blue arrowheads indicate crista and IBM, respectively. Scale bar=500nm. (D)Zoomed-in multicolored Lookup Table (LUT) from (C), showing the  $\Psi_m$

as a heat map, where white and blue pixels represent the highest and lowest  $\Psi_m$ , respectively. Scale bar  $\frac{1}{4}$ 500nm. Using the Nernst equation, we show that the crista (white arrowhead) in the middle of the mitochondrial section has a membrane potential of 181.6mV relative to the cytosol ( $\Psi_{Cr-Cyt}$ ), whereas this crista has a membrane potential of 23.7mV relative to its proximal IBM (blue arrowhead) ( $\Psi_{\alpha-IBM}$ ). The histogram (lower left) shows the membrane potential of cristae regions compared to neighboring IBM regions when using the average mitochondrial membrane potential of the whole organelle as a reference. Error bars indicate standard deviation. This demonstrates that  $\Psi$  associated with cristae ( $\Psi_{Cr}$ ) tends to be above, whereas as  $\Psi$  associated with IBM ( $\Psi_{IBM}$ ) tends to be below, that of the average membrane potential of the entire mitochondrion. Statistical analysis was performed on individual cristae within zoomed-in region. Note that the heterogeneity among different cristae indicates that each crista displays a degree of electrochemical autonomy from its neighbors.